JOURNAL OF SPACECRAFT AND ROCKETS
Vol. 43, No. 1, January–February 2006

Spatial and Temporal Correlation of Spacecraft Surface Charging in Geosynchronous Orbit

H. Koons* and J. Mazur†
The Aerospace Corporation, El Segundo, California 90245
A. Lopatin‡
INTELSAT, Washington, D.C. 20008
D. Pitchford§
New Skies Satellites N.V., 2517 KR The Hague, The Netherlands
and
A. Bogorad¶ and R. Herschitz**
Lockheed Martin Commercial Space Systems, Newtown, Pennsylvania 18940

Surface-charging sensors are used on spacecraft to measure the potential between a sample material on the surface and the spacecraft frame. The frame is taken to be electrical ground. A study has been performed to determine how far away a surface-charging sensor can be in local time in geosynchronous orbit and still provide reasonable situational awareness about hazardous surface-charging conditions to a nearby spacecraft. The study was conducted using surface-charging sensor data from four INTELSAT and two New Skies Satellites communications satellites and electron temperature data from one electrostatic analyzer provided by Los Alamos National Laboratory for a spacecraft in geosynchronous orbit. The distances between pairs of nearby spacecraft covered a range from 5.5 to 34 deg in longitude or 0.4 to 2.3 h in local time. We have cross-correlated data from pairs of spacecraft for two large surface-charging events in April and July 2000 and also plotted scatter diagrams of the data for pairs of vehicles for the entire year 2000. For the two large events we find a relatively high, normalized, cross-correlation coefficient indicating a significant degree of temporal correlation with time lags varying from 0 to 22 min. When looking at scatter diagrams from many more events over a one-year period, we find no apparent organization in the data. There appears to be no obvious relationship between the potentials measured simultaneously on adjacent vehicles during charging events. We also found no amplitude correlation between the electron temperature measured on one vehicle and the surface potential measured on another located only a few degrees away in longitude. However, individual charging events are usually (but not always) encountered within the same time period on nearby spacecraft. We conclude that surface potential measurements for the purposes of anomaly diagnosis or situational awareness of potentially hazardous environmental conditions cannot be made on nearby vehicles but must be made on each spacecraft in geosynchronous orbit.

I. Introduction

A STUDY has been conducted to determine the spatial and temporal correlation of spacecraft surface charging in geosynchronous orbit. When anomalies occur on spacecraft in the plasma sheet during times of moderate to high geomagnetic activity, they are often blamed on electrostatic discharges cause by surface charging. Surface-charging sensors are used on spacecraft to measure the potential difference between a sample material on the surface and the spacecraft frame. The frame is taken to be electrical ground. This potential difference is called the surface potential or sample potential. Particle sensors can measure the potential difference between the spacecraft frame and the surrounding plasma. This potential difference is called the frame potential. Both types of sensors have been used to diagnose surface-charging hazards. The sensors used for this diagnosis are frequently on spacecraft located several hours away in local time. This diagnosis is rarely made using data from sensors on the spacecraft experiencing the anomaly because few spacecraft carry such sensors onboard. We have used sensors on spacecraft located relatively close together to determine the dependence of surface charging on the separation between the spacecraft. For this purpose we have used surface potential data from charging plate analyzers (CPA) on four INTELSAT spacecraft, identified as 801, 802, 804, and 805, and two New Skies Satellites (NSS) spacecraft, identified as 803 and 806, and electron data from a Los Alamos National Laboratory's magnetospheric plasma analyzer (MPA) on a geosynchronous spacecraft. The separation between pairs of spacecraft used in this study covered a range from 6 to 34 deg in longitude or 0.4 to 2.3 h in local time in geosynchronous orbit.

We have previously shown that CPA sensors with surface normals pointing in the direction away from Earth reliably indicate when a surface-charging environment is present at the spacecraft's location when the sensor is shadowed by the body of the spacecraft, that is, when the vehicle is located between 18:00 and 06:00 local time (LT).[1] We also showed that there is an apparent correlation between the temporal charging profile measured by the CPA and the electron temperature profile measured by the MPA on a nearby spacecraft for a few selected charging events in 1998 and 1999.

Here we report the results of a much more comprehensive study that examined more closely the dependence of surface charging on the separation of the sensors.

Received 12 May 2004; revision received 15 February 2005; accepted for publication 25 February 2005.

*Distinguished Scientist, Space Science Department, Space Science Applications Laboratory, 2350 E. El Segundo Boulevard. Member AIAA.
†Manager, Space Science Department, Space Science Applications Laboratory, 2350 E. El Segundo Boulevard.
‡Operations Manager, 3400 International Drive, NW.
§Staff Spacecraft Systems Engineer, Rooseveltplantsoen 4.
¶Senior Staff Engineer, Specialty Engineering Group, 100 Campus Drive.
**Manager, Specialty Engineering Organization, 100 Campus Drive.

II. Instrumentation

The CPAs on the INTELSAT and NSS spacecraft consist of 2×2 in. (5.1×5.1 cm) aluminum plates with Chemglaze dielectric paint on their external surface. They are bonded to the outer surface of the spacecraft with a nonconducting adhesive. The control electronics are located inside the body of the spacecraft. Each sensor measures the potential difference between the surface of the paint and the spacecraft frame. The circuit is described by Bogorad et al.[2] There are two CPA sensors on each vehicle. The sensor referred to as the $-z$ (minus z) sensor always faces away from the Earth. The y sensor faces north on the 805 and 806 vehicles and south on the other four. We have limited our analysis to the $-z$ sensors because the y sensors are continuously illuminated by sunlight during part of each year and also because they exhibited some anomalous behavior, possibly related to structures on the spacecraft.

The $-z$ sensors provide reliable results when they are in darkness from approximately 18:00 to 06:00 LT. One-minute resolution data were used for the study. We have not considered differences between eclipse and sunlight charging because there is no significant difference in either the average and or the worst-case charging levels measured by the CPA when the spacecraft are in sunlight or when they are in eclipse. Surface charging around midnight is not identifiably different from pre- and postmidnight charging. The average surface-charging potential occurs at about 0245 LT. The average falls relatively smoothly to small values at the dawn and dusk terminators. The most negative values encountered when examined in hourly bins are quite uniform from 2100 to 0700 LT.

The MPA instruments measure the three-dimensional plasma electron and ion distributions. The MPA is a spherical-sector electrostatic analyzer. Six separate but contiguous detectors cover the total field of view. In one spin period the MPA views ~92% of the unit sphere. While the spacecraft spins through 15 deg in azimuth, the MPA plate voltage is swept through 40 logarithmically spaced energy channels ranging from ~40 keV/e down to ~1 eV/e. In 86 s the instrument cycles through one three-dimensional electron distribution and two three-dimensional ion distributions. The instrument is further described by Bame et al.[3] During data reduction, the raw three-dimensional count matrices from the detectors are first converted to electron and ion distribution functions. Moments of these functions are then calculated for high- and low-energy electrons and ions. In this paper we compare surface charging measured by the CPA with the electron temperature perpendicular to the geomagnetic field calculated for the high-energy electron range which is ~30 eV to 40 keV.

During some surface-charging events, the potential of the spacecraft frame with respect to the plasma can be determined from the ion measurements. When the vehicle is negatively charged and there are very low-energy ions present in the ambient plasma, these low-energy ions are accelerated across the plasma sheath surrounding the vehicle. A line then appears in the ion energy spectrum at the energy corresponding to the potential drop across sheath. We have found that the frame potential derived from the ion measurements is not a very reliable indicator for surface charging. The measurement yields a reasonable potential only when there are cold ions present in the plasma. However, most spacecraft surface charging occurs in the plasma sheet where the ion temperature is high and no cold ions are present.

The CPA and MPA represent two different measuring techniques for determining periods when spacecraft surface charging is occurring. The CPA measures the potential difference between a surface sample and the spacecraft frame. The MPA measures the potential difference between the spacecraft frame and the surrounding the plasma. Even on the same spacecraft these two types of measurements do not give the same results during periods of surface charging.

Figure 1 shows data from three instruments on the SCATHA spacecraft during a charging event on 23 April 1981 (Ref. 4). The top panel shows the spacecraft frame potential with respect to the plasma. These data were obtained from the acceleration of low-energy ions across the plasma sheath as measured by the Sheath Electric Fields instrument.[5] This measurement is similar to the MPA

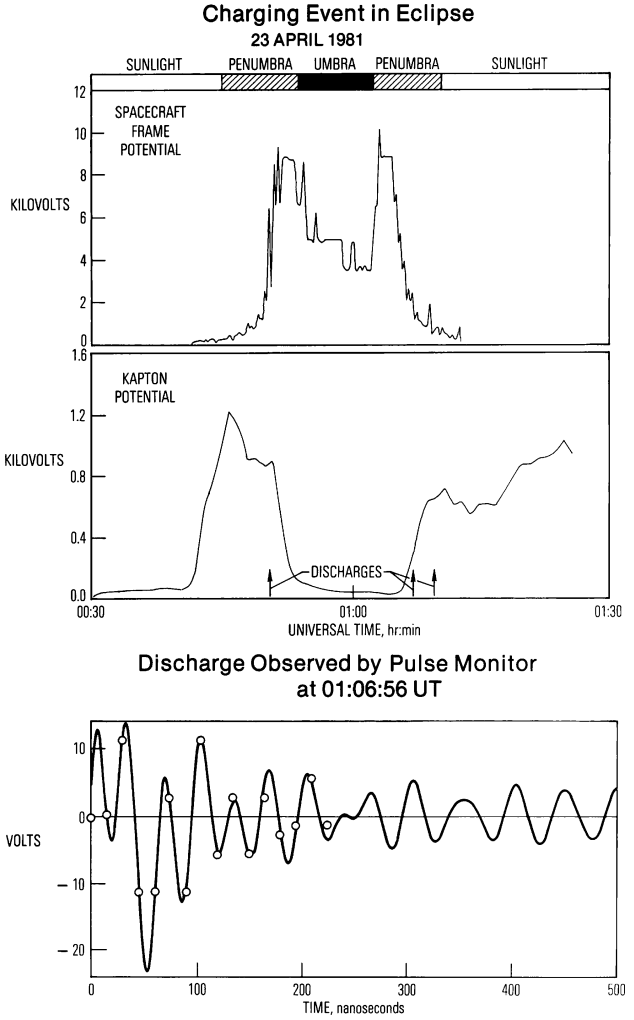

Fig. 1 Spacecraft charging event observed by the SCATHA spacecraft during a substorm near local midnight on 23 April 1981: top, spacecraft frame potential with respect to the ambient plasma measured by an electrostatic analyzer; middle, Kapton sample surface potential with respect to the vehicle frame; bottom, pulse shape for the first discharge identified in the middle panel. The sign of the potentials in the top and middle panels is negative.

technique. The middle panel shows the potential of the surface of a dielectric Kapton sample with respect to the spacecraft frame. These data were obtained by one of the satellite surface potential monitors on SCATHA.[5] This measurement is similar to those made by the CPA although the technique is quite different. Three electrostatic discharges detected by the pulse analyzer[5] occurred during this event at the times indicated by the arrows at the bottom of the middle panel. While this charging event was in progress, an eclipse of the sun occurred at the spacecraft. A bar at the top of the figure shows the times of the vehicle passage through the penumbra and umbra.

The charging event started while the vehicle was in sunlight. The Kapton potential abruptly increased above 0.1 kV (negative), and the frame potential just began to register a potential (also negative) signaling the beginning of the event. The electrostatic analyzer indicated that the vehicle encountered hot plasma-sheet plasma at that time. As the sunlight diminished, the spacecraft frame began to charge, and the surface potential of the Kapton sample began to drop with respect to the frame. One discharge occurred in the first penumbral crossing before the frame potential had charged significantly. The event continued with very little correlation between the potential of the frame and the surface potential of the Kapton sample. There is also no clear correlation between the time of the discharges and the time of potential maxima for either measurement or the time of the maximum rate of change of either potential. In general the discharges tended to occur when the surface potential

of the Kapton sample was relatively high and the frame potential was relatively low. This observation suggests that neither surface- nor frame-potential measurements can be used as precise indicators of the times when discharges might occur. Rather, they can only identify time periods when charging events are in progress and provide an estimate of the severity of the events. Differential charging is a necessary condition for achieving the breakdown electric field required for surface discharges. But the charging of the frame might not occur especially if a significant portion of the frame is exposed to sunlight. The overall process is obviously complex. Here we report on a study of a very large number of events using both types of detectors on nearby spacecraft.

III. Accuracy and Intercalibration of the CPA Sensors

The CPA sensors on the INTELSAT and NSS spacecraft were designed, constructed, and installed on essentially identical spacecraft and expected to be identical in performance. However, it was noted that the cumulative frequencies of occurrence of the CPA potentials for the six vehicles differed substantially even during quiet times.[1] For example, during 119 quiet days when the Planetary Magnetic Index, Kp, was less than 2, the CPAs on vehicles 803–806 measured potentials more negative than −300 V fewer than 1% of the time. This never happened on 801, but happened 5% of the time on 802. The cumulative frequency of occurrence of the charging voltage for the CPAs on all of the vehicles for the period from 18:00 to 06:00 LT (the night hemisphere) for all of 2000 is shown in Fig. 2. This shows that, for all but the very largest potentials, the sensor on 801 measures systematically the lowest negative voltage and the one on 802 measures the highest negative voltage when negative potentials are present. The different statistical responses suggest that the accuracy of the measurements is much less than the precision inherent in the electronics. This can be caused by differences in the paint thickness, differences in the materials surrounding the sensors, or differences in the calibrations. The exact cause is unknown. We believe that the statistical responses over a period as long as one year should be about the same with possible differences only at the extremes. Because of this inaccuracy in the measurements, we have performed an in-flight intercalibration of the sensors by normalizing the cumulative frequency distributions of the CPA voltages from the six sensors. The cumulative frequency distributions for the night-side data for the year 2000 are shown in Fig. 2. From Fig. 2 we see that charging is detected about 20% of the time on each vehicle. We do not know what causes the positive potentials below the 0.1% occurrence level. Many of these occur for a brief period of time when the vehicle crosses the dawn terminator into sunlight.

We chose the sensor on 806 to be the standard sensor and normalized the data from the sensors on the other vehicles to that one. We performed this intercalibration by plotting the sample values from

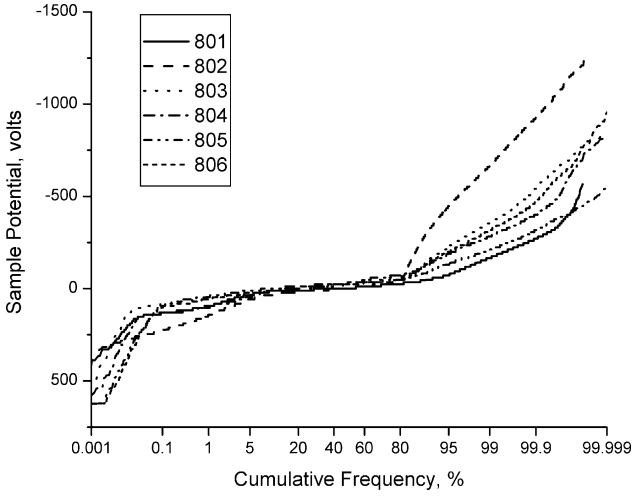

Fig. 2 Cumulative frequency of occurrence for the CPA sample potentials measured on six spacecraft during 2000 for the hours between 18:00 and 06:00 LT.

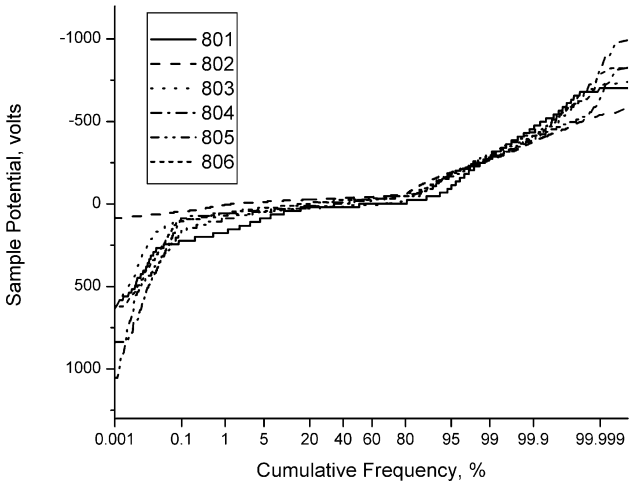

Fig. 3 Cumulative frequency of occurrence for the CPA sample potentials measured on six spacecraft during 1999 and calibrated using the calibration coefficients obtained from the 2000 data.

the vehicle to be calibrated against the sample values from 806 at the following eight levels of cumulative frequency of occurrence: 80, 85, 90, 95, 99, 99.9, 99.99, and 99.999. These values cover the range of the potentials when charging was occurring. These curves were then fit with nth-order polynomials. Reasonable fits were obtained for fifth-order polynomials for 801, 802, and 803 and third-order polynomials for 804 and 805. The extrapolation of the fit was not reasonable beyond a frequency of 99.999 for the sensor on 802.

Although third- and fifth-order polynomials were used to give accurate fits, the dominant terms by far were the first and second, that is, the dc offset and the gain. These both had quite large variations among the sensors. The relative dc offset from 806 ranged from −28.9 to +104 V, and the relative gain varied from 0.35 to 5.8.

As a verification of this intercalibration procedure, we tested the cumulative frequency distributions for the year 1999 using the polynomial coefficients from the calibrations obtained from the 2000 data. The results are shown in Fig. 3. Each of the curves in Fig. 3 contains over 500,000 points. There is good agreement among the curves for all but the extreme values indicating that there are no significant calibration changes from 1999 to 2000. The extreme values most likely differ because the vehicles were not all exposed to the same extreme environments.

The following is an example of the accuracy of the data before and after intercalibration. Before calibration (Fig. 2) at 95 percentile, the average potential was -210 ± 129 V. After calibration (Fig. 3) at 95 percentile, the average potential was -164 ± 36 V. The lower average value after normalization is consistent with a reduction in the levels for the 806 vehicle and indicates that the charging levels were generally lower in 1999 than in 2000.

IV. Correlations of Signals on Nearby Vehicles

In 2000 the spacecraft were located around geosynchronous orbit as shown in Fig. 4 (Ref. 1). We have correlated the signals from the four closely spaced vehicles 801, 803, 805, and 806. Table 1 shows the approximate spacing in local time between pairs of these vehicles.

We first examine the correlation of the data for two of the largest charging events in the sense that they produced extremely large potentials on at least one of the four vehicles. The two largest charging events measured by 803 during the entire data set, covering the time period from 9 October 1997 through 31 October 2002, occurred on 7 April and 15 July 2000. The largest event occurred on 15 July with a peak negative potential of −1126 V at 20:29 UT (19:03 LT). The second largest occurred on 7 April with a peak negative potential of −1118 V at 00:53 UT (23:29 LT). The two events are expected to have different temporal profiles at the vehicles because the 15 July event occurred at dusk and the 7 April event occurred near midnight. One of these two events appeared in the top 20 events list for the

Table 1 Separation in local time and geocentric angle between vehicle pairs in geosynchronous orbit

Vehicle pair	Separation in local time, min	Separation in angle, deg
804-L97A	22	5.5
801-806	36	9.0
801-803	40	10.0
805-806	60	15.0
803-806	76	19.0
801-805	96	24.0
803-805	136	34.0

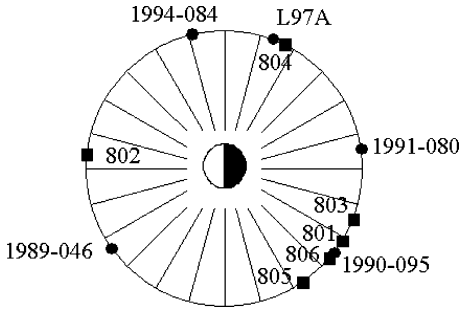

Fig. 4 Satellite locations at 00:00 UT in November 1998: ■, INTELSAT and New Skies Satellites with CPAs and ●, satellites with LANL MPAs.

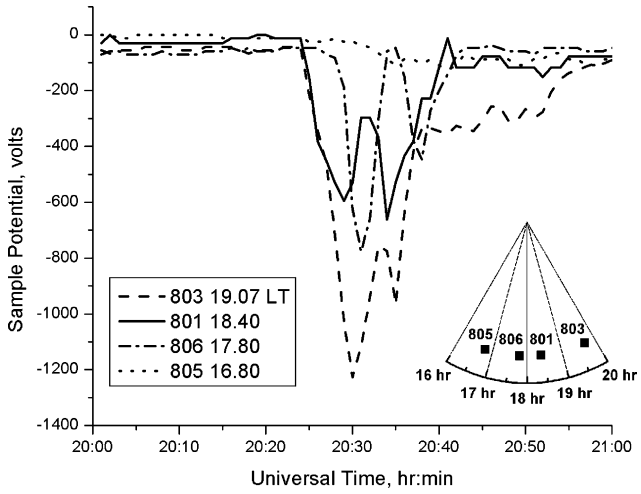

Fig. 5 Sample potential as a function of time from the CPA sensors on 15 July 2000. The legends give the locations of the satellites in local time at 20:30 UT.

same time period for all of the other nearby vehicles. The 15 July event was #7 for 801 and #6 for 806. The 7 April event was #7 for 805. In general, large events are seen by all of the nearby vehicles, but there is no direct relationship between their rankings in intensity.

Figure 5 shows the time-history profile of the CPA surface potentials for the four vehicles during the 15 July charging event. The largest negative potential was measured on 803. The peak potentials on 801 and 806 were roughly a factor of two lower. The event was quite small on 805. However, the $-z$ sensor on 805 was still exposed to sunlight when the peak negative potential was measured on 803. The y sensor was also exposed to sunlight because it reported a positive potential throughout this entire charging period.

We have performed cross-correlation and linear regression analyses of the data for each pair of vehicles for this event. The normalized cross-correlogram of the potentials for the pair {801, 806} is shown in Fig. 6a. The normalization for each pair was computed by dividing the cross-correlation function by the square root of the autocorrelation functions of each potential at zero time displacement. Negative time displacement signifies that the signal at the

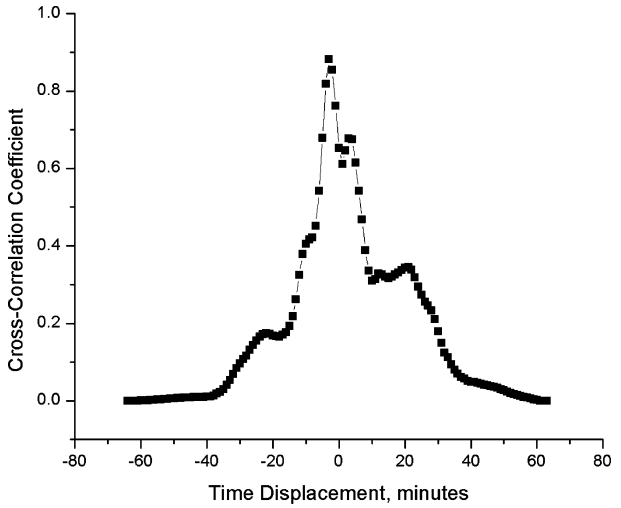

Fig. 6a Normalized cross-correlogram for the sample potentials from the CPA sensors on 801 and 806. Negative time displacement signifies that 801 leads 806.

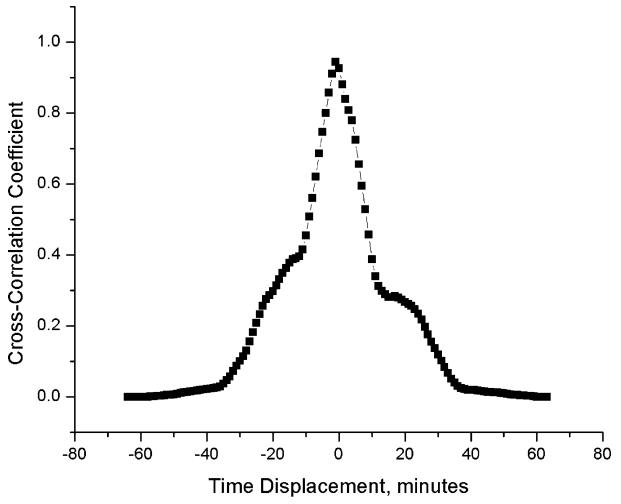

Fig. 6b Normalized cross-correlogram for the sample potentials from the CPA sensors on 801 and 803. Negative time displacement signifies that 801 leads 803.

first vehicle in the braces occurs before the signal at the second. In Fig. 6a the sample potential from 801 leads the sample potential from 806 by 3 min. The normalized cross-correlogram for the pair {801, 803} is shown in Fig. 6b. This pair has the highest correlation coefficient, 0.94, at a time lag (negative time displacement) of 1 min. The cross-correlation coefficients and the time displacements of the maxima for all of the pairs are given in Table 2. The table also gives the full width at half-maximum of the cross-correlogram. This is a measure of the correlated time duration of the events. In this case it was about 19 min at {801, 803} and {803, 806} but only 8 min at {801, 806}. This suggests that the injected plasma did not flow over the constellation of satellites in an orderly way from either east to west or west to east.

The second method we have used to obtain a measure of the degree of correlation between the data from pairs of vehicles is the coefficient of correlation determined from the variation of the sample potentials around a regression line. Figure 7a is a scatter diagram of the sample potentials from 806 plotted against the sample potentials from 801 for the time period from 20:00 to 21:00 UT on 15 July, 2000. The sample potentials from 806 have been advanced by 3 min with respect to those from 801 to account for the temporal cross-correlation results shown in Fig. 6a. The solid line is the regression line. The dotted line is the regression line expected if the sample potentials measured at the two vehicles were identical. The regression

Table 2 Cross-correlation results for the 15 July 2000 surface-charging event

Vehicle pair	Maximum cross-correlation coefficient	Time displacement of maximum,[a] min	Full width at half-maximum, min	Linear regression coefficient
801-806	0.88	−3	8	0.82
801-803	0.94	−1	19	0.90
803-806	0.85	−10	19	0.76

[a]Negative time displacements indicate that the signal from the first vehicle of the pair leads that of the second.

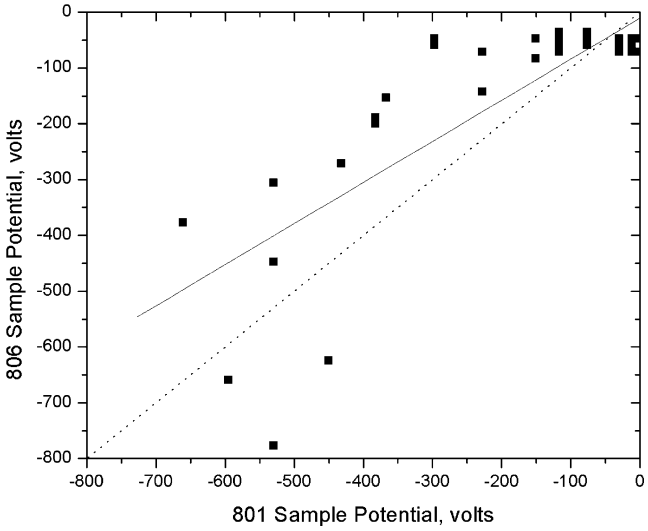

Fig. 7a Scatter diagram of the sample potential from the CPA sensor on 806 against the sample potential from the sensor on 801 during the charging event on 15 July 2000. The regression coefficient for the fit is $R = 0.82$, and the standard deviation is 91 V.

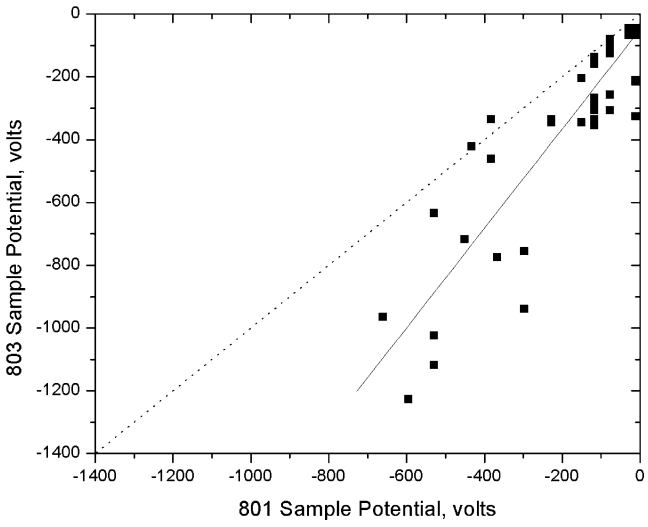

Fig. 7b Scatter diagram of the sample potential from the CPA sensor on 803 against the sample potential from the sensor on 801 during the charging event on 15 July 2000. The regression coefficient for the fit is 0.91, and the standard deviation is 130 V.

line being above the line of equality shows that the sample potentials on 806 are generally greater (in the signed sense) than the sample potentials on 801. The coefficient of correlation r is given in the last column of Table 2. A similar scatter plot for the sample potentials from 803 plotted against the sample potentials from 801 is shown in Fig. 7b. The sample potentials from 803 have been advanced by 1 min with respect to those from 801 to account for the temporal cross-correlation results shown in Fig. 6b. Here the regression line is below the line of equality signifying that the sample potentials

Table 3 Cross-correlation results for the 7 April 2000 surface-charging event

Vehicle pair	Maximum cross-correlation coefficient	Time displacement of maximum,[a] min
801-805	0.81	−2
803-806	0.72	0
805-806	0.90	+1
801-803	0.74	+14
801-806	0.77	+16
803-805	0.70	+22

[a]Negative time displacements indicate that the signal from the first vehicle of the pair leads that of the second.

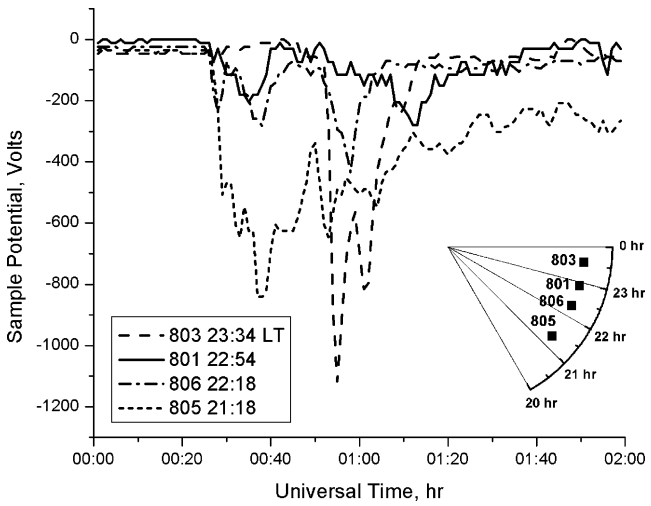

Fig. 8 Sample potential as a function of time from the CPA sensors on 7 April 2000. The legends give the locations of the satellites in local time at 01:00 UT.

on 803 are generally lower than those on 801. Taken together with the coefficients of determination in Table 2, the results in Figs. 6 and 7 show that there is, at best, a mediocre correlation in time and amplitude between pairs of vehicles. The amount by which the regression lines in Fig. 7 depart from the lines of equality shows that there is a poor correlation between the absolute amplitude of the surface potentials measured on pairs of vehicles. This is true even when the time difference of the event as seen by the two vehicles is accounted for as it is in Fig. 7.

The sample potentials for the four nearby vehicles for the charging event on 7 April 2000 are shown in Fig. 8. For this event the most negative potential for 803 is −1118 V, and it occurred at 23:29 LT. The normalized cross-correlogram of the potentials for all of the vehicle pairs is shown in Fig. 9. The correlation coefficients for each of the pairs and the time lags of the dominant peak for each pair are given in Table 3. Both the time profiles and the cross-correlograms show a much more complex structure for the April event than they did for the July event. The relatively large values at the maximum for the normalized correlation coefficients for each of the pairs mean that the events have considerable temporal correlation for each of the pairs.

Scatter diagrams for this event for pairs of vehicles, such as the example shown in Fig. 10, show little linear correlation between the amplitudes of the potentials measured at the two vehicles. At any given time there appears to be little if any relationship between the potentials measured at any pair of vehicles.

We have also looked at the correlation between vehicle pairs over a much longer period. A scatter diagram for the potentials seen on the pair {801, 803} for the year 2000 is shown in Fig. 11. Only points for which the potential measured on at least one of the vehicles was more negative than −300 V are plotted. The lack of any apparent organization in the plot clearly shows that there is no relationship between the surface potentials measured simultaneously on closely spaced vehicles.

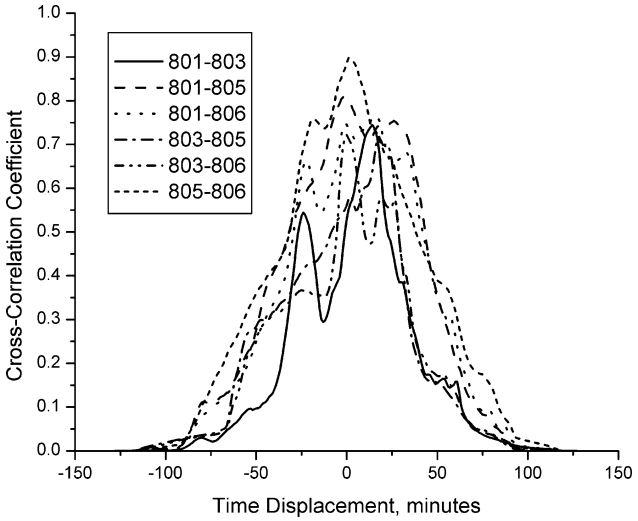

Fig. 9 Normalized cross-correlograms for the sample potentials measured by the CPA sensors for all of the vehicle pairs for the charging event on 7 April 2000.

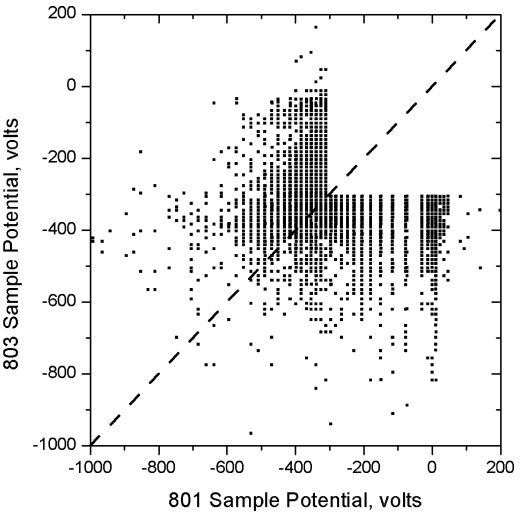

Fig. 11 Scatter diagram of the sample potential from the CPA sensor on 803 against the sample potential from the sensor on 801 during the hours from 18:00 to 06:00 LT for all of the year 2000. Only points for which the potential was more negative than −300 V on at least one of the sensors are plotted.

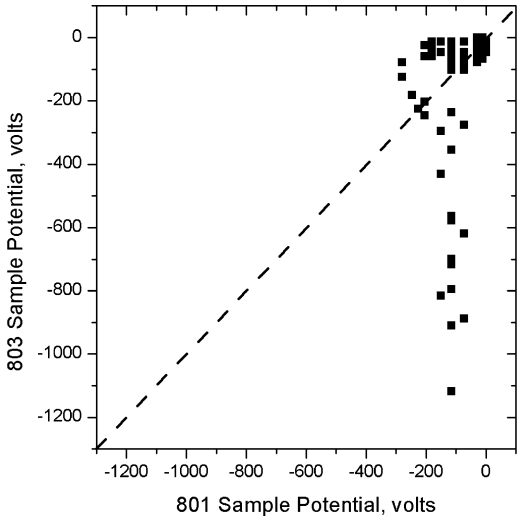

Fig. 10 Scatter diagram of the sample potential from the CPA sensor on 803 against the sample potential from the sensor on 801 during the charging event on 7 April 2000.

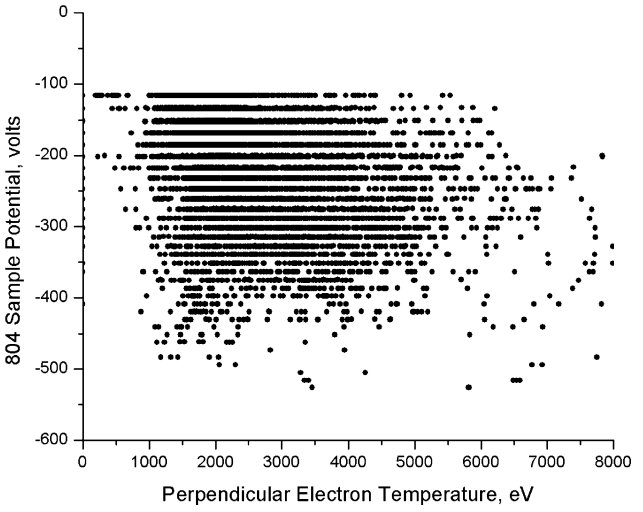

Fig. 12 Scatter diagram of the sample potential from the CPA sensor on 804 against the electron temperature determined from MPA measurements perpendicular to the local magnetic field during the hours from 18:00 to 06:00 LT for all of the year 2000. Only points for which the potential was more negative than −100 V are plotted.

V. Comparisons of CPA with MPA Measurements

Vehicle 804 was located quite close to LANL-97A in 2000 as shown in Fig. 4 and Table 1. We have compared the CPA sample potentials on 804 with the perpendicular temperature of the electrons and with the spacecraft frame potential measured by the MPA on LANL-97A. Garrett et al.[6] reported an earlier attempt to compare energetic electron-flux measurements on 1976-059A, a geosynchronous spacecraft that flew particle sensors provided by the Los Alamos Scientific Laboratory, and the frame potential measured on ATS 6. Those spacecraft flew within 500 km of each other, and the measurements were reported for a 10-day period when their separation was less than 7 deg in longitude. They found that they had sufficient information to "make an adequate estimate" of the maximum frame potential to which ATS 6 charged.

Because the sampling rates for the data are different on 804 and LANL-97A (once every 60 s for the CPA and once every 86 s for the MPA), we have rounded the times to the nearest minute and plotted only those data points for which data are available for both measurements at the same minute. We also only consider times when the CPA sample potential is more negative than −100 V. The scatter diagram of the MPA perpendicular electron temperature as the independent variable and the CPA sample potential as the dependent variable is shown in Fig. 12. There is no evident relationship between the two variables.

We have also correlated the sample potentials on 804 with the spacecraft frame potentials measured by the MPA on LANL-97A. The results are similar to the scatter shown in Fig. 12.

We conclude that the surface-charging parameters measured essentially simultaneously by different techniques on the two nearby vehicles have little correlation with one another.

VI. Situational Awareness

Because few spacecraft today are instrumented to monitor surface potentials or frame potentials, there is a desire to use instruments on nearby spacecraft to warn or diagnose when hazardous conditions are present. We have used the CPA data in two studies to test the efficacy of such a scheme.

Table 4 Results of the first situational awareness study

Sensor	Client	ΔLT, h	Client events	Warnings	Correct warnings,[a] %	False alarms,[a] %	Failures to detect,[b] %
801	806	0.60	5559	4313	26	74	80
806	801	0.60	4313	5559	20	80	74
801	803	0.67	3056	4313	12	88	83
803	801	0.67	4313	3056	17	83	88
801	805	1.60	4804	4313	17	83	85
805	801	1.60	4313	4804	16	84	83
805	806	1.00	5559	4804	30	70	74
806	805	1.00	4804	5559	26	74	70
803	806	1.27	5559	3056	42	58	77
806	803	1.27	3056	5559	23	77	38
803	805	2.27	4804	3056	18	82	88
805	803	2.27	3056	4804	12	88	82

[a]The correct warnings and the false alarms are given as percentages of the number of warnings.
[b]The failures to detect are given as percentages of the number of client events.

A situational-awareness color scale was developed for charging events. The data consist of the 1-min samples of the CPA sample potentials from the nearby vehicles 801, 803, 805, and 806. They cover the time period from 8 October 1997 to 31 October 2001. Only surface potentials more negative than −100 V were considered. On this scale potentials more negative than the 97th-percentile level are considered the most hazardous because they are the most severe events. They are colored red. The frequency levels for this scale are based on frequencies for the National Oceanic and Atmospheric Administration scale for geomagnetic storms. The 97th percentile is used because that corresponds to the frequency of strong, severe, and extreme geomagnetic storms as determined by the Planetary Magnetic Index, that is when Kp = 7, 8, and 9 (Ref. 7). As an example, on 801 the red level extends from −383 V to the lowest observed level of −1022 V. For the first study for each pair of vehicles, we considered one vehicle to be the sensor vehicle supplying the data and the other to be the client vehicle using the data. Thus the client vehicle receives the hazard warning from the sensor vehicle. Table 4 shows the results for all combinations of pairs among the four vehicles. In Table 4 the column labeled Warnings gives the number of samples measured above the 97th percentile by the sensor vehicle.

It is clear from the small percentage of correct warnings compared to the large percentages of false warnings and failures to detect that the use of sensors on nearby spacecraft, even those as close as 30 to 40 min in local time, is unacceptable for any application such as anomaly diagnosis where it is necessary to know whether large surface-charging levels are present at the client vehicle essentially at the same time that a measurement is made at the sensor vehicle. The previous analysis showed that within the sample measurement timescale of 1 min there is essentially no correlation between the sensor values at nearby vehicles.

In the second study we looked at somewhat longer time periods by examining the 20 largest charging events seen by the sensor on 801 and determining when the sensors on 806 and 803 responded to the same events. We defined an isolated severe charging event to be a charging event with at least three contiguous minutes with the sample voltage above the 97th-percentile charging level. The requirement for three contiguous minutes excludes the occasional noise signal above the red level and also the occasional signal above the red level when a preponderance of signals is below the red level. An isolated event ends when the sample voltage falls below the 97th-percentile level. For 801, isolated severe events had durations ranging from 3 to 161 min. We define a long severe charging event to be a set of isolated severe charging events with a gap of less than 1 h between isolated events.

The results for the 20 long charging events containing the most negative sample voltages are given in Table 5. They are listed in the order of the local time of the start of each event from dusk (1800 h LT) to dawn (0600 h LT). The list is limited to those events that occurred between 15 March 1998 and 31 October 2001 when simultaneous data were available from all three vehicles. The total number of isolated events on each of the vehicles during that time period was 287 on 801, 412 on 803, and 331 on 806.

In Table 5 the event no. in the first column is the severity of the event from number 1, the event with the most negative sample voltage on 801 to number 20, the event with the least negative sample voltage of the 20 most severe events. The 20 long charging events on 801 actually include many more isolated charging events. In fact they contain all of the 35 largest isolated events that occurred during the March 1998 through October 2001 time period. The remaining columns are in sets of four. They show the number of minutes when the sensor on the vehicle identified at the top of the column reported a red level during each of the four 10-min periods beginning 20 min before the start of an event on 801 and ending 20 min afterward. If T is the time of the start of an event on 801, the four 10-min periods are T − 11 to T − 20, T − 1 to T − 10, T to T + 9, and T + 10 to T + 19. An N in the column signifies that no charging event with a sample voltage lower than −100 V occurred during the time period.

The following observations can be made about the charging events on closely spaced vehicles from the data in Table 5:

1) The most severe events above the red level have only a few isolated precursors in the red. Except for a few isolated minutes, the sensor on 801 (whose data are shown in the middle set of columns) measured a red level only 12 min out of a possible 400 min during the 20-min period before the start of a severe red event.

2) No charging at all can be present on nearby spacecraft during a red event at a nearby vehicle. For example, no charging at all occurred on 803, and only charging below the red level occurred on 806 during the 20 min after the strongest event started on 801 (event no. 1).

3) Some charging with levels below the charging threshold voltage of −100 V usually occurred on the client vehicles throughout the 20 min after the onset of a red event on 801. The exceptions are event nos. 1 and 9 on 803 when no charging occurred at all.

4) Some charging with levels below the charging threshold voltage of −100 V usually occurred on the client vehicles throughout the 20 min before the onset of a red event on 801. The exceptions are event nos. 6, 9, 12, and 14 on 806 and 1, 9, and 10 on 803 when no charging occurred at all.

5) Occasionally severe events are already in progress on the client vehicles before a warning could be given by 801. Examples are event nos. 2 and 7 on both 803 and 806. In these two cases the vehicle in the middle was the last to respond to the event.

6) The extreme events tend to occur near local midnight. Four of the five most severe events (event nos. 1, 2, 4, and 5) started between 2330 and 0141 LT.

7) Other than that mentioned in item 6, there is no strong tendency for the most severe charging onsets to correlate with local time.

8) As shown by the sums at the bottom of the columns in Table 5, the number of occurrences of red levels is remarkably the same for 803 and 806 for the different time periods before and after the onset on 801 and differs markedly from the sums for 801. The only obvious difference is that the events were chosen because they were the onsets for the most severe events on 801.

For situational awareness and hazard warnings it is useful to determine how accurate warnings using the sensor on 801 would be

Table 5 Number of minutes each CPA sensor vehicle is charged to the red (97th percentile) level during the two 10-min periods before and after a red event starts at vehicle 801

		806 (west)				801 (center)				803 (east)			
Event no.[a]	LT[b]	−20	−10	+10	+20	−20	−10	+10	+20	−20	−10	+10	+20
6	1819	N[c]	N	3	2	0	0	7	2	0	0	9	2
7	1822	7	10	10	2	0	2	8	0	9	7	9	0
3	2124	2	1	7	10	0	0	8	0	0	7	2	0
14	2153	N	N	1	2	0	0	6	10	0	7	6	8
16	2156	0	0	0	0	0	1	10	4	0	0	2	0
10	2219	0	0	3	7	0	1	6	8	N	N	0	5
12	2222	N	N	0	1	0	0	10	4	0	0	3	0
18	2259	0	1	6	5	0	0	10	6	0	0	0	0
2	2330	10	8	10	10	0	2	10	10	5	5	10	10
4	0059	0	0	0	0	0	0	7	7	0	0	4	9
17	0107	0	0	0	0	3	2	10	2	0	0	0	0
1	0135	6	0	0	0	1	0	8	9	N	N	N	N
5	0141	0	3	8	0	0	0	10	10	0	1	9	9
9	0243	N	N	0	0	0	0	10	10	N	N	N	N
13	0315	0	0	8	10	0	0	10	10	0	0	2	0
20	0320	0	6	6	0	0	0	10	1	0	0	9	7
8	0340	0	0	7	5	0	0	10	10	0	0	1	8
15	0356	0	0	5	0	0	0	10	10	0	0	0	0
11	0446	0	0	0	9	0	0	10	10	0	1	6	8
19	0524	0	0	10	10	0	0	10	10	0	0	9	7
Sum	——	25	29	84	73	4	8	180	133	14	28	81	73

[a]The event no. in column 1 is the order of the severity of the event (most negative sample voltage measured during the event) on 801.
[b]The events are ordered by the local time (column 2) of the 801 spacecraft at the start of the event.
[c]An N indicates that the sample level was above −100 V (not charged) during that entire 10-min period.

Table 6 Results of the second situational awareness study[a]

Result	806 (west)		803 (east)	
Correct warning	9	45%	9	45%
False alarm	4	20%	5	25%
Failure to detect	7	35%	6	30%

[a]The number of events are given for each category for each client vehicle followed by the percentage of the 20 events used in the study.

for the client vehicles, 803 and 806. We define a correct warning to be a warning with no red levels on a client vehicle for the preceding 20 min, for example, event nos. 6 and 19 on 806. We define a false alarm to be a warning that is not followed on a client vehicle by a red level during the succeeding 20 min, for example, event nos. 8 and 14 on 803. We define a failure to detect to be a warning that occurs after a red level has occurred on a client vehicle during the preceding 20 min. The results are shown in Table 6. The results for the leading (803) and trailing (806) vehicles are remarkably similar. Although the number of correct warnings is two to four times higher that those found in the first study, at less than 50% they are too low to provide more than a very general situational awareness of the charging environment.

VII. Conclusions

We conclude that surface potential measurements for the purposes of anomaly diagnosis or situational awareness of potentially hazardous environmental conditions must be made on each spacecraft in geosynchronous orbit. Because the SCATHA observations show that neither surface potential measurements nor frame potential measurements alone give an adequate picture of surface charging, we recommend that both types of measurements be made with simple instruments on each vehicle. We have found that the frame potential derived from the ion measurements is not a very reliable indicator for surface charging. However, the two techniques together provide a more comprehensive view of the interaction of the spacecraft with the environment, and when both are available and are measuring hazardous levels the confidence level in a diagnosis of surface charging is increased. We also recommend that pulses on each spacecraft be monitored with a discharge detector. Only the simultaneous measurements of hazardous surface potentials and corroborating frame potentials with the occurrence of a discharge provide reliable information that the natural space environment caused an anomaly that can be attributed to surface charging.

Acknowledgments

The authors wish to express their gratitude to Michelle Thomsen and Geoffrey Reeves of the Los Alamos National Laboratory for providing the data from the magnetospheric plasma analyzer and for discussions and comments that significantly improved the manuscript. This work was supported in part by The Aerospace Corporation by a contract from INTELSAT, in part by The Aerospace Corporation Independent Research and Development Program, and in part by NASA Grant NAG5-10938.

References

[1]Ozkul, A., Lopatin, A., Shipp, A., Pitchford, D., Mazur, J. E., Roeder, J. L., Koons, H. C., Bogorad, A., and Herschitz, R., "Initial Correlation Results of Charge Sensor Data from Six INTELSAT VIII Class Satellites with Other Space and Ground-Based Measurements," *Proceedings of the 7th Spacecraft Charging Technology Conference*, SP-476, ESA, Noordwijk, The Netherlands, 2001, pp. 293–298.

[2]Bogorad, A., Bowman, C., Dennis, A., Beck, J., Lang, D., Herschitz, R., Buehler, M., Blaes, B., and Martin, D., "Integrated Environmental Monitoring System for Spacecraft," *IEEE Transactions on Nuclear Science*, Vol. 42, No. 6, 1995, pp. 2051–2057.

[3]Bame, S. J., McComas, D. J., Thomsen, M. F., Barraclough, B. L., Elphic, R. C., Glore, J. P., Gosling, J. T., Chavez, J. C., Evans, E. P., and Wymer, F. J., "Magnetospheric Plasma Analyzer for Spacecraft with Constrained Resources," *Review of Scientific Instruments*, Vol. 64, No. 4, 1993, pp. 1026–1033.

[4]Koons, H. C., "Summary of Environmentally Induced Electrical Discharges on the P78-2 (SCATHA) Satellite," *Journal of Spacecraft and Rockets*, Vol. 20, No. 5, 1983, pp. 425–431.

[5]Stevens, J. R., and Vampola, J. R., "Description of the Space Test Program P78-2 Spacecraft and Payloads," The Aerospace Corp., SAMSO TR-78-24, El Segundo, CA, Oct. 1978.

[6]Garrett, H. B., Schwank, D. C., Higbie, P. R., and Baker, D. N., "Comparison Between the 30- to 80-keV Electron Channels on ATS 6 and 1976-059A During Conjunction and Application to Spacecraft Charging Prediction," *Journal of Geophysical Research*, Vol. 85, No. A3, 1980, pp. 1155–1162.

[7]"NOAA Space Weather Scales," National Oceanographic and Atmospheric Administration Space Environment Center, User Notes, Issue 28, Boulder, CO, Jan. 2000.

A. Ketsdever
Associate Editor